EARTHQUAKE ENGINEERING AND STRUCTURAL DYNAMICS
Earthquake Engng Struct. Dyn. 2000; **29**:359–376

Estimation of soil shear modulus softening during strong ground shaking using ground surface and downhole acceleration recordings

R. O. Davis*

Department of Civil Engineering, University of Canterbury, Christchurch, New Zealand

SUMMARY

An algorithm for estimating the average shear modulus for a soil site containing a downhole accelerometer array is described. For distant or weak earthquakes, the usual procedure for estimating shear modulus is to perform time-series correlation of two downhole records. The vertical distance between instruments divided by the peak correlation lag time gives the average shear wave velocity. The shear modulus follows easily. This method is not applicable for stronger earthquakes where non-linear softening effects lead to progressively slower shear wave velocities. The method presented here overcomes the softening effect by compressing the time scale of the upper acceleration record. Time compression is accomplished in such a way that the peak correlation of the two records is maximized. The algorithm steps through the records, maximizing the correlation peak by adjusting the time scale within an active time interval. The resulting compressed upper record can be interpreted as the ground motion that would have occurred had softening not taken place. The summation of the various time scale adjustments shows both the amount of softening and the time at which it occurred. Copyright © 2000 John Wiley & Sons, Ltd.

KEY WORDS: downhole arrays; shear modulus; shear wave velocity; softening; cross-correlation

INTRODUCTION

Vertical arrays of accelerometers spaced at intervals of 10–20 m have been placed at a number of sites throughout the world [1–4]. They are generally referred to as downhole arrays. Their central purpose is to provide direct measurement of site amplification effects. The resulting acceleration records from different depths provide valuable insight into the propagation and modification of seismic waves in the site soils. Interpretation of data from a recorded event is relatively

* Correspondence to: R. O. Davis, Department of Civil Engineering, University of Canterbury, Private Bag 4800, Christchurch, New Zealand

Contract/grant sponsor: New Zealand Earthquake Commission Research Foundation; contract/grant number: 99/345

Received 23 July 1998
Revised 29 June 1999
Accepted 24 August 1999

straightforward for small or distant earthquakes where the ground deformation is relatively small and elastic behaviour predominates. In these cases investigators normally model the soil response using vertically propagating SH waves. There is a requirement of course for shear moduli values in order to specify shear wave velocities. Estimates of shear modulus for the soils involved may be obtained by several means including laboratory tests, field seismic profiling, or time-series correlation of the downhole records themselves.

Shear moduli are not so easily estimated for stronger earthquakes when softening due to non-linear soil behaviour may introduce unwanted complications. In stronger events the site soils may undergo progressive changes depending on the levels of stress and strain and (for saturated soils) pore pressure increase. It is not nearly so easy to estimate shear moduli for these circumstances. Clearly field seismic profiling is inappropriate as only small strain deformations are involved. Laboratory tests can be adapted to simulate the estimated stress history, but there are obvious difficulties in synthesizing an appropriate stress history and then implementing it in the lab.

Often, time-series correlation of downhole acceleration records from two depths has been used to estimate the average velocity of waves propagating between those depths. The time-series correlation directly provides an estimate for the lag or travel time for waves to propagate from the lower depth to the higher. The wave velocity is obtained by dividing the distance between instruments by the peak correlation lag time. Wave velocities can then be easily translated into modulus values. This method is clearly appropriate, provided the level of ground motion is not sufficiently strong to result in significant non-linear soil behaviour. As an example, Elgamal *et al.* [4] used time-series correlation for a variety of small earthquakes to assess the shear wave velocity structure at the SMART1 Lotung downhole test site in Taiwan. The data developed in [4] were later used in the analysis of stronger motion data from larger earthquakes at the test site [5].

Problems arise with correlation of records when stronger levels of shaking occur. In those cases, early parts of the acceleration history will correspond to the generally stiffer small deformation moduli values that initially exist at the site. As shaking progresses the moduli may soften and the wave travel time between the instrument locations in the downhole array will lengthen. This lengthening may be significant whenever the shaking is sufficiently strong to generate non-linear effects. If one now correlates the two entire records, the calculated lag will reflect neither the initial small deformation behaviour nor the later softened behaviour. Instead one obtains an average lag lying somewhere between the initial and softened values. Several investigators have used a variety of methods to overcome this difficulty. Resonant frequencies determined from Fourier spectral ratios were used by Chang *et al.* [6] to estimate shear wave velocities at the Lotung SMART 1 array. A similar analysis was carried out by Wen *et al.* [7]. In a separate efforts, Li *et al.* [8] employed a sophisticated hypoplasticity model to numerically simulate ground motion at the Lotung site, while Kazama [9] directly approximated shear stress and strain for the Kobe Port Island downhole acceleration records. None of these methods enjoy the simplicity and directness associated with simple correlation of two downhole records.

This paper attempts to overcome the problem described above. Consider the typical two-instrument downhole array sketched in Figure 1. It is desired to obtain a continuous history of shear wave velocity (or the corresponding shear modulus) throughout the times where shaking and softening occur. We will present a technique for compressing the time scale of the upper acceleration time history in such a way as to precisely counteract the effects of softening. The new, compressed acceleration history will represent the soil response without softening effects. Its

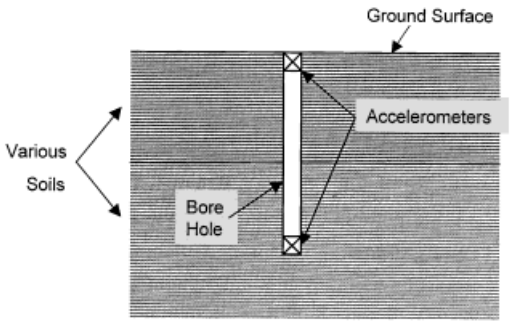

Figure 1. Typical downhole accelerometer array.

correlation with the buried instrument record will approximate the small deformation response of the intervening soils just as would be the case if no softening had occurred. Meanwhile, the amount of time compression suffered by the upper record will tell us how much softening has occurred and when it occurred. It will be possible to construct a complete picture of the average shear wave velocity between the two instrument levels throughout the duration of the earthquake.

There are several possible applications for the softened shear modulus history. One can directly compare field softening data with published models for shear modulus reduction such as given by Seed *et al.* [10]. In instances where liquefaction has been observed, the softening history may give considerable insight into both the onset of liquefaction and the later solidification process. Comparison and verification of analytical site amplification models are possible as well.

The algorithm developed below is quite robust. It provides as much detail as the user requires, consistent with the time scale for the acceleration records and the distance between the downhole instruments. The method will be illustrated by considering a case history in which extreme amounts of softening occurred: the downhole acceleration records from the Port Island array at Kobe.

BACKGROUND

The basic elements of our method are most easily described by reference to specific downhole records. Therefore, we begin by considering the Kobe Port Island East–West accelerations from the 0 and 16 m depths illustrated in Figure 2. The aim of our analysis is to estimate the average shear modulus, or equivalently the shear wave velocity, in the upper 16 m, *continuously* throughout the earthquake. Liquefaction was observed at this site and it is clear significant softening occurred during the earthquake.

The full 60 s of shaking shown in Figure 2 is difficult to consider in detail because of the small time scale necessitated by the size of the figure. A more informative picture is developed if we expand the time scale. This has been done in Figure 3 where the time interval between 12 and 20 s has been isolated. It is clear from this figure that marked correlation exists between the two records. The wave crests denoted A, B and C strongly suggest upward propagating shear waves that, with only minor changes of wave form, move from the 16 m depth to the soil surface.

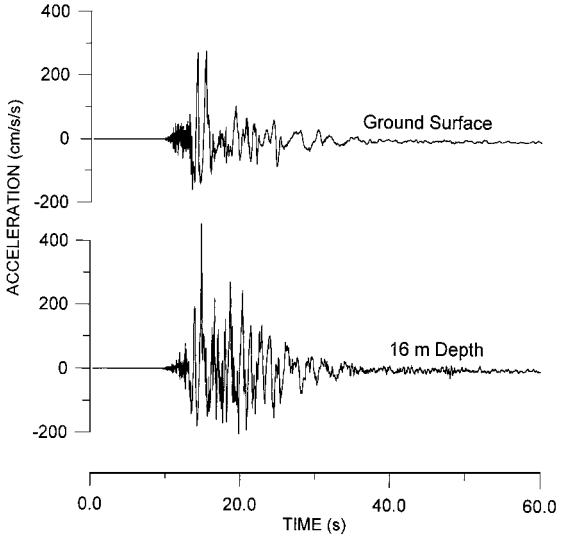

Figure 2. Kobe Port Island acceleration records. East–West data from 0 and 16 m depths.

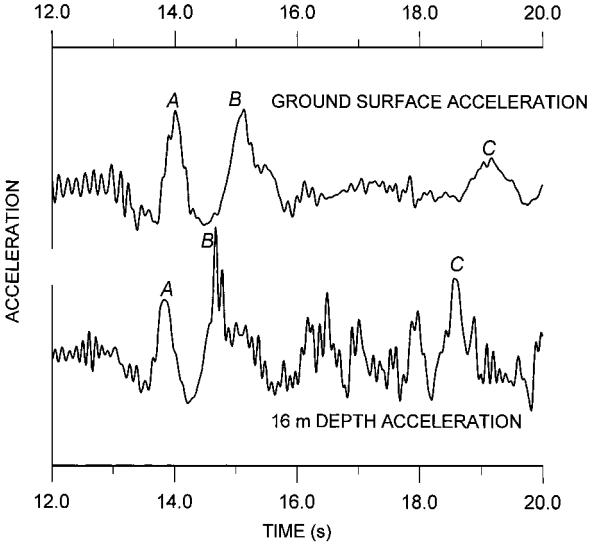

Figure 3. Expanded segment of data from Figure 2.

However, closer inspection shows that the lag times associated with the three wave crests are significantly different. Examining the digitised records, we find the lag for peak A is 0.17 s, for peak B it is 0.46 s, and for peak C, 0.61 s. The increasing time lag results from the extreme softening of the site during the time interval shown in Figure 3.

We can attempt to better understand the Kobe response by examining the correlation of the two records. The discrete-time series correlation of two sampled functions $a_k = a(t_k)$ and $b_k = b(t_k)$ is defined as [11]

$$\Gamma(t_m) = \sum_k b_{k+m} a_k \tag{1}$$

where the sum is taken over the entire record. Often Γ is given in normalised form,

$$\Gamma_n(t_m) = \frac{\Gamma(t_m)}{(\sum_k a_k^2)^{1/2} (\sum_k b_k^2)^{1/2}} \tag{2}$$

Direct calculation of Γ using Equation (1) can be seriously time consuming for long records. In practice, one uses the discrete correlation theorem which states that Γ is one member of the discrete Fourier transform pair

$$\Gamma(t_k) \Leftrightarrow B_k A_k^* \tag{3}$$

Here A_k and B_k are the discrete Fourier transforms of a_k and b_k and $*$ denotes complex conjugation. A_k and B_k are found using fast Fourier transforms of the given data. The inverse FFT is then used to find Γ. The resulting calculation is extremely efficient.

The functions Γ and Γ_n will both show a peak at the value of t_k corresponding to the lag or time delay between the two records. The normalized correlation for the two Kobe records is shown in Figure 4. We see a strong peak at $t = 0.31$ s. This is the calculated lag for the two records. The corresponding shear wave velocity is 16 m/0.31 s = 51.6 m/s. This value is, at best, an average wave velocity for the entire time interval of the record. It cannot represent the softening behaviour of the site soils as shaking progresses.

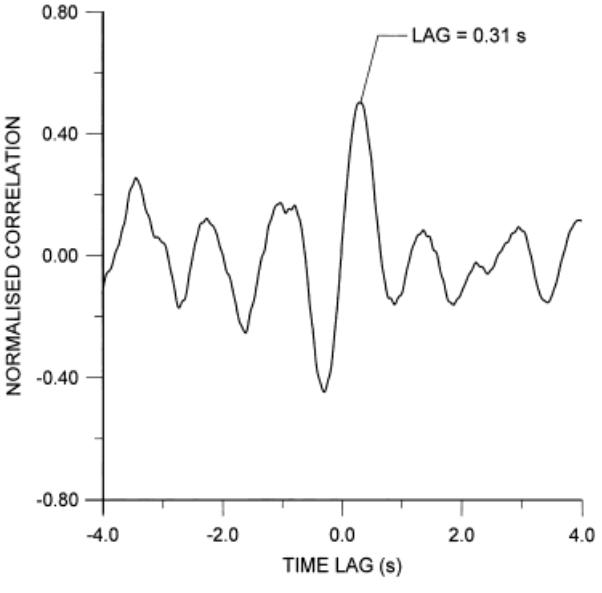

Figure 4. Normalized correlation of East–West Port Island records.

One approach to dealing with softened records such as Kobe is to break down the two records into distinct windows and consider the individual correlations for each window. This was done for the Kobe records by Elgamal *et al.* [12]. Their results indicate a dramatic reduction in soil stiffness, but lack fine detail regarding the continuous variation of shear wave velocity or shear modulus. The basic problem with this method lies in the size of the record segments to be used. The segments must be sufficiently large to be representative of some part of the record. The resulting lag is a single number associated in some (not fully specified) way with the segment. If the segment is made too small, the desired correlation will often be lost and spurious values for the lag may result. We will compare this method with the proposed algorithm later in the paper.

ANALYSIS

Our aim here is to use the correlation of two records as a tool to lead to a continuous picture of the shear wave velocity. The idea is to maximize the correlation by non-linearly compressing the time scale of the upper acceleration record. Referring again to Figure 3, it is clear that compressing the time scale of the upper record in some appropriate way could lead to better correlation of the two records. If the correct amount of time compression were put in place, the increasing lag associated with wave crests B and C could be completely eliminated and all three peaks could have the same lag. The effect on the correlation function Γ shown in Figure 4 would be twofold: first the peak at 0.31 s would be shifted to the left, second the magnitude of the correlation peak would be increased. This suggests that we could use the magnitude of the peak value of Γ as a criterion for adjusting the time scale of the upper record.

Next, we realize that if the time scale is compressed, the amount of compression necessary to maximize the correlation will be equal to the amount by which softening of the site soil has lengthened the travel time between the two instruments. If we divide the distance between the instruments by the sum of the travel time for small deformation elastic waves plus the amount of time compression, the result should be the shear wave velocity corresponding to the softened soil profile. This is the basic idea of our analysis.

In more detail, we proceed as follows. Suppose we have two sampled acceleration records denoted a_k and b_k such as those shown in Figure 2. Let a_k be the record from the higher instrument. Also, let the time corresponding to a_k and b_k be t_k, and assume the time increment δt between samples is a constant. Now, consider a new time scale denoted $\hat{t}_k$ where time is compressed in some segment of the record. We define $\hat{t}_k$ as follows:

$$\hat{t}_k = \begin{cases} t_k & \text{for } t_k \leqslant t_S \\ t_k - \Delta\left(\dfrac{t_k - t_S}{t_F - t_S}\right) & \text{for } t_S < t_k \leqslant t_F \\ t_k - \Delta & \text{for } t_F < t_k \end{cases} \tag{4}$$

Here $\hat{t}_k$ is the compressed time, t_S and t_F are the start and finish times for the compressed segment, and Δ is the total amount of compression at the end of the segment. Time is compressed linearly between t_S and t_F and we continue throughout the remainder of the record using a constant time translation Δ. An example of a compressed time scale is shown schematically in Figure 5. In the figure the compression Δ has been taken as 0.50 s and the values of t_S and t_F are 14.0 and 16.0 s. The new compressed time is shown by the solid line while the dashed 45° line is simply a plot of

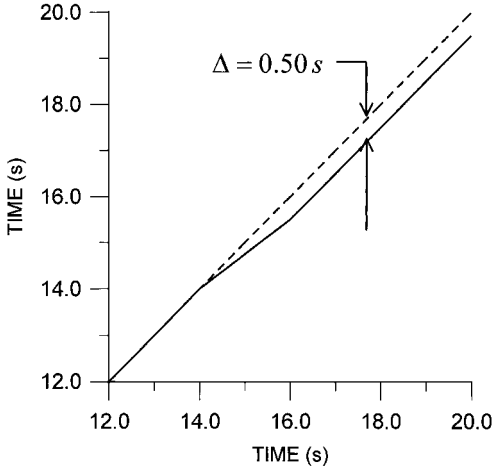

Figure 5. Example of compressed time scale.

the original time versus itself. Note that the new compressed time $\hat{t}_k$ will no longer have a constant increment size δt on the interval $[t_S, t_F]$ and the values of $\hat{t}_k$ and t_k will generally be different for all times greater than t_S.

Next, we rewrite the upper acceleration record, interpolating the values of acceleration at the appropriate times in the newly compressed time scale. In this way, we realign the new compressed acceleration record with the original sampling times. This is necessary in order that we can carry out the correlation of the new record with the original b_k acceleration record. We rewrite the record as follows. For any desired value of time t_j in the original time base, we find the corresponding acceleration using linear interpolation

$$\hat{a}_j = a_k + (a_{k+1} - a_k)\left(\frac{t_j - \hat{t}_k}{\hat{t}_{k+1} - \hat{t}_k}\right) \tag{5}$$

Here $\hat{a}_j$ is the new interpolated acceleration at time t_j, $\hat{t}_k$ is compressed time, a_k is the acceleration corresponding to $\hat{t}_k$. The index k is selected so that $\hat{t}_k \leqslant t_j \leqslant \hat{t}_{k+1}$. It is a simple matter to sweep through the compressed record interpolating the new acceleration values. The results of this effort are new accelerations based on the compressed time scale, but now properly aligned with the original time base. An example is illustrated in Figure 6. The time interval for compression is defined by $t_S = 14.0$ s and $t_F = 16.0$ s. For purposes of illustration, the value of Δ has been set equal to 0.25 s. In practice, the value of Δ will be determined by maximising the correlation. Also, the interval to be compressed will generally be considerably shorter than 2 s, but a large value is useful to illustrate the concepts involved. In Figure 6 the dashed line is the original acceleration record and the solid line the compressed record. Note how the compression is initiated at $t_S = 14.0$ s and how the amount of compression remains constant for times greater than $t_F = 16.0$ s.

Our algorithm for estimating shear wave velocity is outlined in Figure 7. We begin by partitioning the time scale for the complete record into M segments $(t_F - t_S)$ of equal size. Then beginning with segment one, we maximize the peak value of the correlation Γ by adjusting the

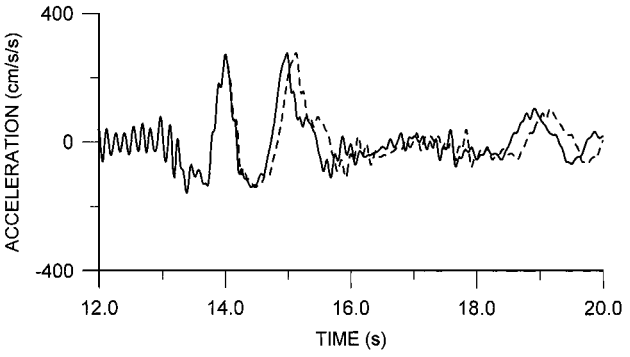

Figure 6. Example of effect of compressed time on ground surface acceleration from Port Island.

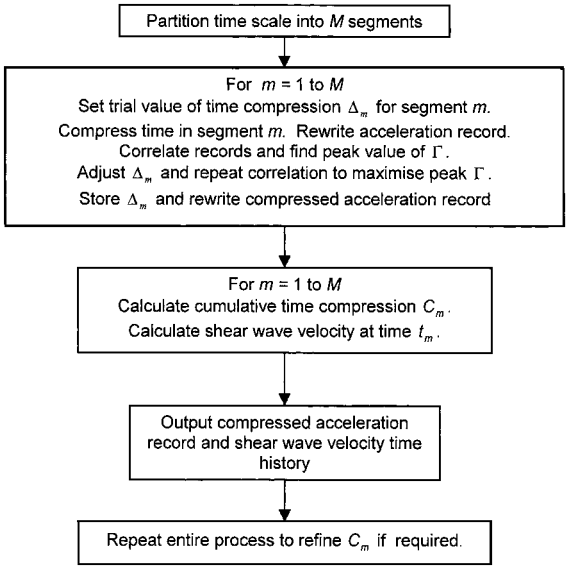

Figure 7. Flow diagram for time compression algorithm.

value of the compression Δ_1. Note that the correlation is made using the entire record. The compression of segment one not only affects the record within the segment but also at all later times. We then move forward to segment 2, maximizing Γ to find Δ_2, and so on through the record, stopping only when the shaking becomes too weak to be of interest or when the values of Δ_m become very small in comparison to the segment size. Next, we note the Δ_m's for each segment have a cumulative effect on all the record that follows. Therefore, we construct the cumulative time compression C_m according to

$$C_m = \sum_{i=1}^{m} \Delta_i, \quad m = 1, 2, \ldots, M \tag{6}$$

The value of C_m represents the time compression required to offset the softening effect caused by strong shaking in the soil up to the time corresponding to the end of segment m.

Once time compression is complete, the two acceleration records will be correlated with a lag time corresponding to the initial small deformation shear modulus of the soil before softening commenced. This lag can be read off the final correlation. Let its value be t_0. We can now construct the shear wave velocity history as

$$v_S(t_m) = \frac{\text{distance between instruments}}{t_0 + C_m} \tag{7}$$

Here t_m denotes the time at the end of segment m.

In the next section we will show a typical application using the Kobe Port Island records. However, before doing this, three points should be noted. The first concerns the problem of optimizing the magnitude of the correlation peak by adjusting the value of the time compression Δ_m for segment m. This is a relatively simple one-dimensional optimization problem. Several different optimizing schemes were tried while the algorithm was under development. The most effective, from the standpoint of being both straightforward and highly stable, was the golden section algorithm. The subroutines GOLDEN and MBRAK from *Numerical Recipes in Fortran* [13] were employed directly. The MBRAK routine first brackets the optimal compression value. Then GOLDEN refines the value to within the desired tolerance. For the Kobe analysis described below, the tolerance was set equal to 0.01 s, the value of the time interval for the acceleration records.

The second point to note here is that the entire algorithm outlined above may be repeated. That is, the fully compressed record emerging at the conclusion of the optimization may be reused as if nothing had occurred. The result is a new cumulative time compression, say C'_m. We may then sum C_m and C'_m to obtain a refined time compression. Experience suggests the best procedure is to first run the algorithm with a relatively large time interval $(t_F - t_S)$ and then to repeat the process with the time interval halved. A third calculation, with $(t_F - t_S)$ halved again, may be performed and so on. At each stage more detail is added to the time compression record.

Our third comment follows from the second. The magnitude of $(t_F - t_S)$ is of considerable significance to the overall result. If we attempt to make the interval $(t_F - t_S)$ too small, we risk overemphasizing the importance of a small segment of the record. For the Kobe records considered below, we used an initial interval $(t_F - t_S)$ of 0.8 s. Halving this to 0.4 s leads to improvement in the degree of detail embodied in the results. Halving again to 0.2 s yields more detail but does not appear to cause significant improvement. A fourth attempt at 0.1 s generates slightly more detail but is of questionable value. It is important to keep in mind that, at best, we can hope for no more than an accurate representation of the *average* shear wave velocity between the depths of the instruments involved. Other effects such as soil layering, P-waves and surface waves have undoubtedly contaminated the records to some extent and use of an excessively small interval $(t_F - t_S)$ may unduly emphasize their importance.

A second problem can also arise when too small an interval $(t_F - t_S)$ is used. As in almost any optimization problem, our objective function (the peak correlation value) has multiple extrema. This is sometimes referred to as the bumpy mattress problem. We seek to smoothly follow one extreme value as the algorithm sweeps through the record, but it is always possible to jump to another nearby peak that may temporarily appear more attractive to the program. It is not difficult to identify this phenomenon since, if it occurs, the lag time will undergo a sudden

dramatic change. We can generally avoid the problem by using larger intervals ($t_F - t_S$) since they will generally encompass sufficient wave complexity to preclude an easy path for the optimization to take to a spurious peak. On the other hand, small intervals may invite a jump to a nearby local extremum. For this reason, as well as the comment above, small time intervals are not recommended.

EXAMPLE: KOBE PORT ISLAND

Consider once again the East–West acceleration records from the ground surface and 16 m depth at Port Island shown in Figures 2 and 3. We have carried out the programme of calculations outlined above using a time interval of 0.8 s. Figure 8 shows the normalized correlation functions Γ_n for the records both before and after time compression. The dashed line in Figure 8 is identical to the correlation shown in Figure 4. The solid line shows the correlation after time compression. From Figure 8, we see that the magnitude of the peak correlation has been significantly improved (from 0.504 to 0.651) by the compression. We also see the lag has been reduced to 0.07 s. This value suggests an initial small deformation shear wave velocity of 16 m/0.07 s = 228 m/s. Figure 9(a) shows the cumulative time compression C_m plotted versus time. The calculation begins at $t = 5$ s, and for a little more than 7 s C_m remains equal to zero. No time compression occurs in this early part of the record. Around 12 s there is a slight *stretching* of the time scale, indicated by the small negative jump in C_m. Then between 13 and 14 s a rapid compression is found. This part of the record evidently contains the most marked softening of the site soils. A second episode of softening is evident at 25 s, but this is followed by a decrease in C_m indicating stretching of the time scale is required by the algorithm. The computation was stopped at 50 s.

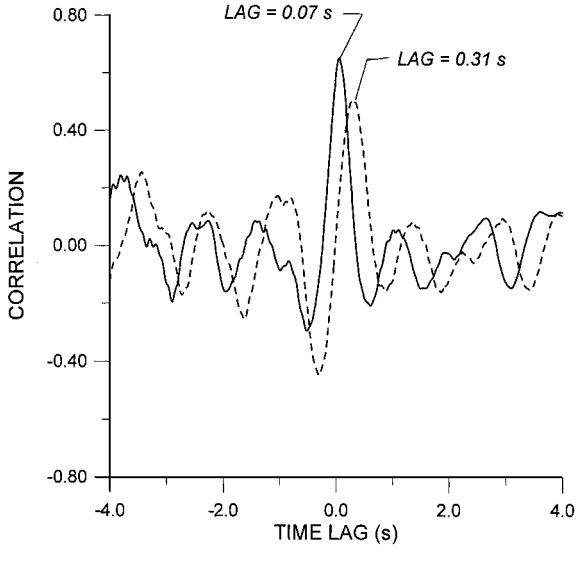

Figure 8. Correlation of Port Island East–West data from 0 and 16 m: dashed line shows correlation of original data; solid line shows correlation after time compression.

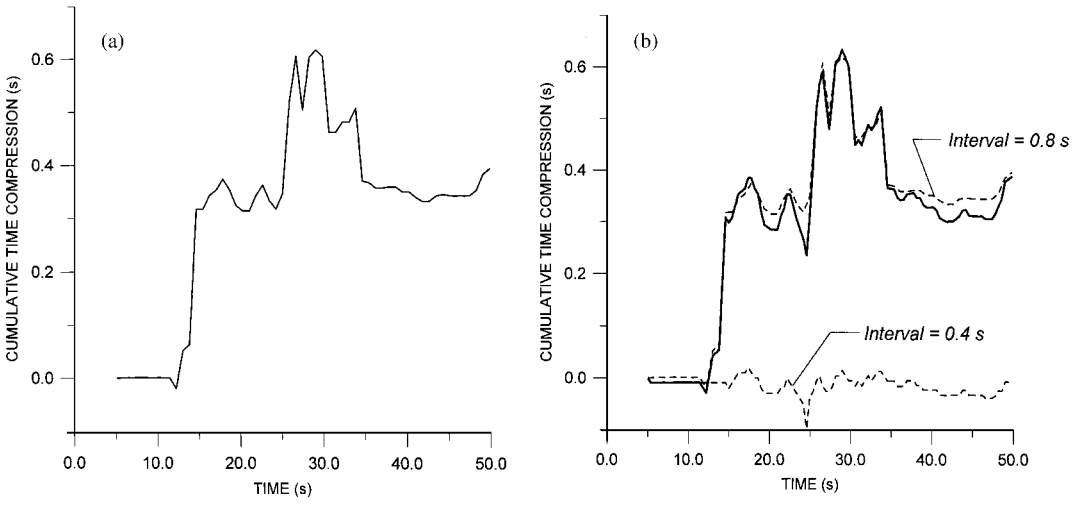

Figure 9. Cumulative time compression for surface acceleration record for Port Island East–West record. (a) Results for 0.8 s intervals. (b) Results after halving the time interval.

Figure 9(b) illustrates the second compression of the record, now using an interval ($t_F - t_S$) of 0.4 s. The compressed upper record from the previous calculation is used as input for this calculation. As one might expect, the resulting time compression is generally small. It is shown by the dashed line hovering around zero compression near the bottom of the figure. The original, 0.8 s interval, cumulative compression is also shown by the second dashed line. The summation of the two lines is shown as the solid line. It seems evident from the figure that additional detail has been added to the original result, but the overall trend in the compression is largely preserved. The magnitude of the peak correlation is increased by this second calculation to a value of 0.692. The lag time remained steady at 0.07 s.

Figure 10 shows the segment of the ground surface acceleration history between 12 and 20 s. The dashed line represents the original acceleration history while the solid line shows the compressed history after the above calculations. Significant amounts of time compression are evident near 14 s. In Figure 11 we have replotted both the upper (compressed) and lower acceleration records, and we have offset the two records by the final lag of 0.07 s. In comparison with Figure 3, it can be seen from this figure how the two records are now visually well correlated.

As we noted above, it is possible to continue repeating the calculation with progressively smaller time increments. Figure 12 illustrates the result of this process for intervals of 0.2 and 0.1 s. The heavy solid line represents the situation following the 0.4 s interval compression. That line is the same as the solid line in Figure 9(b). The dashed line shows the result from the 0.2 s compression and the light solid line shows the 0.1 s calculation. Inspecting the figure we see the smaller time intervals tend to exaggerate some of the peaks in the earlier result. The degree of exaggeration is not large, yet one must doubt their validity for the reasons discussed above. The peak correlation is not greatly increased by either of the new calculations. Its value increases to 0.704 for the 0.2 s run, and to 0.706 for the 0.1 s calculation. The lag time remained steady at 0.7 s throughout both calculations.

As mentioned above, another approach to our problem is individually correlating the two records over individual time windows. Figure 13(a) shows results from such a computation. The

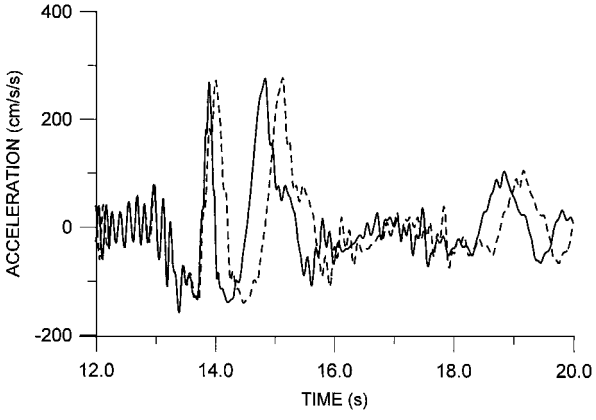

Figure 10. Part of the ground surface acceleration record before and after time compression.

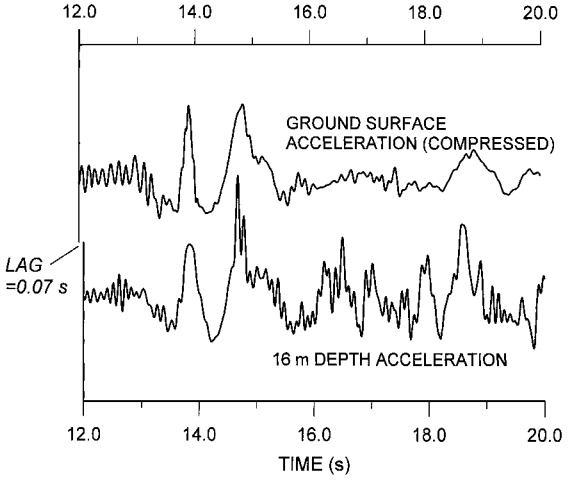

Figure 11. Comparison of 0 and 16 m East–West records after time compression of upper record. Here the 16 m record is offset by 0.07 s.

diamond-shaped data points on the figure represent lag times associated with correlations for a window of 6.4 s duration moving across the entire record. Each of the data points results from correlating the two acceleration records over the time window and then plotting the lag versus the time at the centre of the window. If one halves the window size to 3.2 s, the results become erratic and many points plot well off the scale of the graph. In order to compare these results with the time compression method, we have biased the data in the figure downward by 0.7 s. This accounts for the time compression results being the *additional* lag time over and above the lag associated with small deformation elastic waves. The time compression result for the interval $(t_F - t_S)$ of 0.4 s is shown by the dashed line on the figure. There are similarities between the two data sets but there are significant differences in the timing of the major softening jumps. We can easily discover

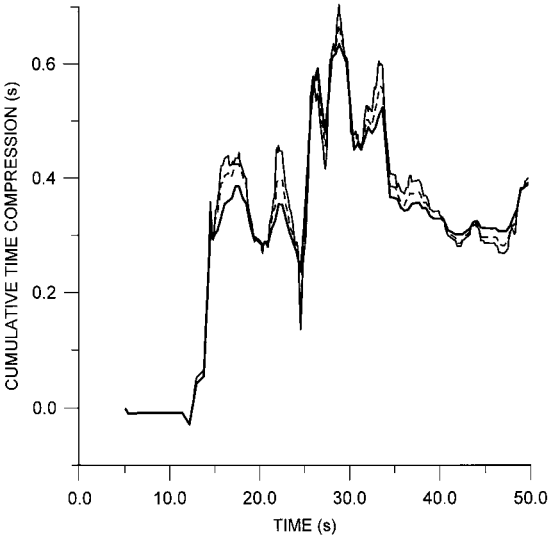

Figure 12. Effect of further halving time interval on cumulative time compression. Heavy solid line is identical to that in Figure 9. Dashed line corresponds to 0.2 s intervals, light solid line to 0.1 s intervals.

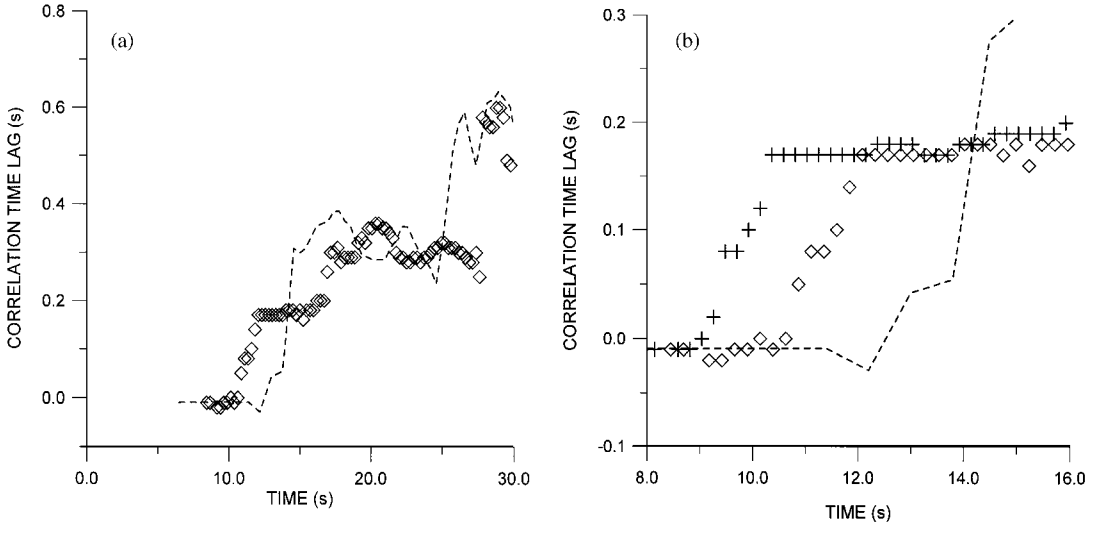

Figure 13. Comparison of time compression and individual window correlation results. (a) Result for 6.4 s window. (b) Comparison of 6.4 s window result (◇) with that for 9.6 s window (+).

the root cause of the differences by performing a second individual correlation calculation using a greater window duration. Results are shown on an enlarged time scale in Figure 13(b). The diamond-shaped data points are identical to those shown in Figure 13(a) for the 6.4 s window. The + data points correspond to the second calculation using a window width of 9.6 s. The

dashed line shows the time compression result. The striking point about this figure is the similar shape but different timing exhibited by the two individual correlation results. The 9.6 s window data show the first strong softening occurring between 9.4 and 10.5 s. The same effect does not appear for the 6.4 s window until roughly 10.7 s, and it ends at about 12 s. The reason for this becomes clear when one inspects the original acceleration records. Referring to Figure 3, note the ground surface acceleration peaks marked *A* and *B*. These occur at roughly 14.0 and 15.1 s. The 6.4 s window will just begin to encompass peak *A* when the centre of the window lies at 14.0 s − 3.2 s = 10.8 s. It will encompass peak *B* when its centre lies at 15.1 s − 3.2 s = 11.9 s. These times almost exactly coincide with the times for the softening indicated by the diamond-shaped points in Figure 13(b). The longer window duration of 9.6 s encounters the peaks somewhat earlier. The exact time difference will be 4.8 s − 3.2 s = 1.2 s, and this is nearly exactly the time separating the two correlation results. It is evident that using individual time windows in this way may lead to flawed understanding. The lag time is dominated by the major peaks of the acceleration record, to the extent that the correlation result is instantaneously skewed as soon as the peak enters the window.

Next, we consider the North–South component for the 0 and 16 m depth instruments. The 12 s − 20 s segment of the North–South acceleration record is illustrated in Figure 14. As before, visual inspection suggests the records are correlated although the correlation is not so clear cut as in Figure 3. If we carry out the time compression algorithm here, the before and after correlation graphs are found in Figure 15. Before time compression the peak correlation lag was 0.37 s. After time compression it is reduced to 0.08 s, slightly larger than the value of 0.07 s found for the East–West records. The cumulative time compression is also somewhat different in this case. It is shown in Figure 16. The East–West cumulative compression from Figure 9 is shown there also as a dashed line. Both results were obtained using the $(t_F - t_S)$ interval of 0.8 s. It is evident from Figure 16 both the North–South and East–West records are in broad agreement. Both suffer dramatic time compression around 14 s and both have a final cumulative compression value near 0.3 s. However, the North–South record does not reveal the dramatic increase and decrease in

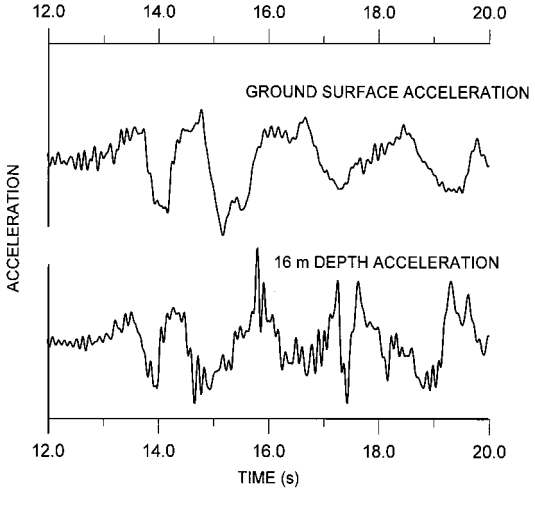

Figure 14. Part of the North–South Port Island acceleration records from 0 and 16 m depths.

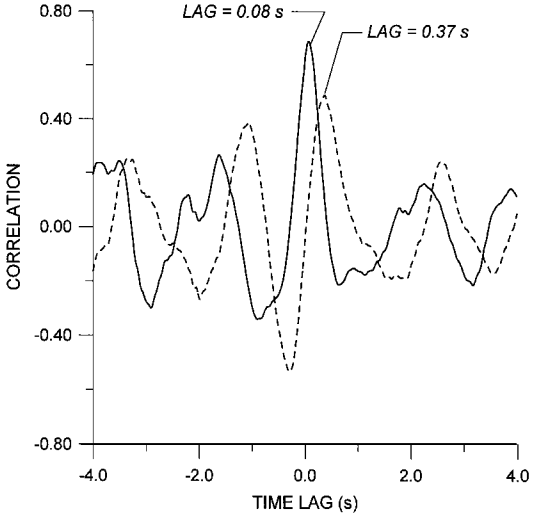

Figure 15. Correlation of Port Island North–South data from 0 and 16 m: dashed line shows correlation of original data; solid line shows correlation after time compression.

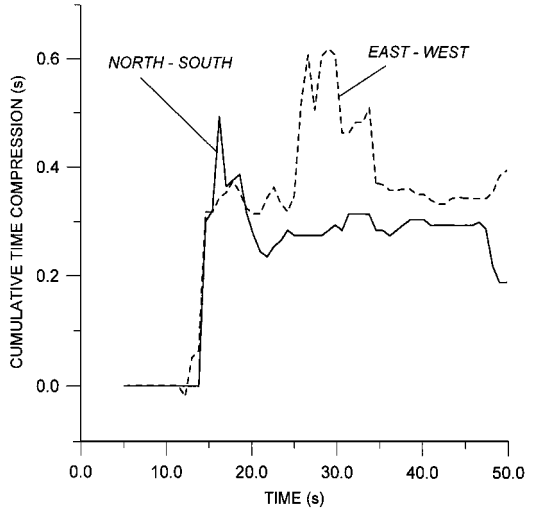

Figure 16. Cumulative time compression curves: solid line for North–South data, dashed line for East–West data.

time compression found between 25 and 35 s on the East–West record. Realising that the cumulative time compression is inversely proportional to the shear modulus, the differences in time compression may suggest anisotropic effects may be present. However, they are of a transient nature, and the soil appears to be more or less isotropic at the conclusion of shaking. This is consistent with the surmise that much of the softening results from increased pore pressure and liquefaction effects.

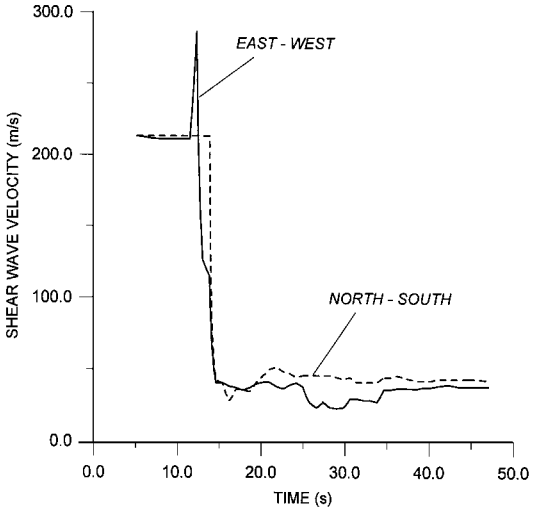

Figure 17. Estimated average shear wave velocity between 0 and 16 m depth at Port Island. Solid line results from East–West records, dashed line from North–South records.

Note that the North–South and East–West records give different estimates for the small deformation elastic lag time. The average of the two values is 0.075 s. Using this average value for t_0, two curves for shear wave velocity based on Equation (7) are shown in Figure 17. The solid line refers to the East–West data, the dashed line to the North–South data. Note the relatively muted effect of the transient jump in time compression between 25 and 35 s on the East–West record. The peculiar spike in the East–West response at about 12 s is caused by the slight time stretching that occurs at that time in Figure 9(a).

This time stretching is not thought to be representative, but it does have a dramatic effect on the shear wave velocity calculation as can be seen from Equation (7). With t_0 equal to 0.075 s, the negative value for C_m equal to -0.019 s results in a shear wave velocity of 286 m/s. This is not considered realistic. We can offer no explanation for the time stretching at 11 s, but it seems highly unlikely stiffening would occur at this point in the record.

Finally, we note that seismic profiling was carried out at the Kobe site to estimate the small deformation shear wave velocity structure. As reported by Iwasaki and Tai [2], the uppermost 5 m soil segment was assigned a velocity of 170 m/s while in the segment between 5 and 19 m the shear wave velocity was found to be 210 m/s. This suggests a small deformation shear wave velocity for the 0–16 m depth of 198 m/s. This value is close to the initial shear wave velocity of 16 m/0.075 s = 213 m/s obtained from the average of the time compression results for the East–West and North–South records.

DISCUSSION

The time compression algorithm presented here possesses several advantages for estimation of shear modulus or shear wave velocity from downhole acceleration records. First, the algorithm is

physically appealing. The idea of time compression bringing the upper acceleration record into closer correlation with the lower is easily grasped and acted on. The algorithm is also computationally efficient. For both the East–West and North–South Port Island records discussed above, the complete calculation time on a 133 MHz Pentium PC did not exceed 150 s. Another advantage is the ability of the algorithm to be used repetitively. If one questions the result of the first time compression computation, a second application will quickly show whether the initial result was accurate or not.

Numerical solutions of optimization problems are often delicate calculations. In the present case we have a large multivariate problem, the dimension of the optimization being equal to M, the number of time intervals for compression. Fortunately, it is not required to *simultaneously* optimise all the Δ_m's; nevertheless, the 'lumpy mattress' effect may still exist for this problem and it may create difficulties in some circumstances. For example, one can envision a pathological situation in which the calculated time compression Δ_m is greater than the segment size. This would imply time is inverted in the segment, not a possibility that could be entertained in any circumstances. Fortunately, the algorithm developed here appears to be quite robust in this regard. The Kobe records clearly represent a severe test, yet the calculations presented above were performed without excessive care and the results appear to be consistent and sensible.

The comparison between time compression and segmental correlation results shows clearly that the two methods are not equivalent. Time compression leads to distinctly different results, and, for the Kobe records, one can argue that time compression gives a significantly more accurate picture of the time at which softening occurred.

Finally, note that Figure 16 shows broad agreement between the East–West and North–South records, particularly near the end of shaking where both calculations suggest little additional softening is occurring. Time compression appears to give a consistent result for both sets of records. Also the small deformation time lags agree closely in both cases, and provide an estimate for the elastic shear wave velocity that is in reasonable agreement with the value obtained from seismic profiling.

ACKNOWLEDGEMENTS

This study was funded by the New Zealand Earthquake Commission Research Foundation under project number 99/345. Grateful thanks are expressed to Dr Yoshinori Iwasaki and the Committee of Earthquake Observation and Research in the Kansai Area (CEORKA) for making the Port Island records available for this study. Thanks are also accorded to two anonymous reviewers of the original version of the paper. Their comments led to significant improvements in computational algorithm.

REFERENCES

1. Ishihara K, Muroi T, Towhata I. In-situ pore water pressures and ground motions during the 1987 Chiba-Toho_Oki earthquake. *Soils and Foundations* 1989; **29**(4):75–90.
2. Iwasaki Y, Tai M. Strong motion records at Kobe Port Island. *Soils and Foundations* (Special Issue: Kobe) 1996; 29–40.
3. Zeghal M, Elgamal A-W. Analysis of site liquefaction using earthquake records. *Journal of Geotechnical Engineering* ASCE 1994; **120**:996–1017.
4. Elgamal A-W, Zeghal M, Tang HT, Stepp JC. Lotung downhole seismic array. I: Evaluation of site dynamic properties. *Journal of Geotechnical Engineering* ASCE 1994; **121**:350–362.
5. Zeghal M, Elgamal A-W, Tang HT, Stepp JC. Lotung downhole array. II: Evaluation of soil nonlinear properties. *Journal of Geotechnical Engineering* ASCE 1994; **121**:363–378.

6. Chang C-Y, Mok CM, Power MS, Tang YK, Tang HT, Stepp JC. Development of shear modulus reduction curves based on Lotung ground motion data. *Proceeding of the 2nd International Conference on Recent Adv. Geotech. Earthquake Engineering Soil Dyns*., St Louis, 1991; 111–118.
7. Wen K-L, Beresnev IA, Yeh YT. Investigation of non-linear site amplification at two downhole strong ground motion arrays in Taiwan. *Earthquake Engineering Structural and Dynamics* 1995; **24**:313–324.
8. Li XS, Shen CK, Wang ZL. Fully coupled site response analysis for 1986 Lotung earthquake. *Journal of Geotechnical Engineering* ASCE 1998; **124**:560–573.
9. Kazama M. Nonlinear dynamic behavior of the ground inferred from strong motion array records at Kobe Port Island during the 1995 Hyogo-Ken Nanbu earthquake. *Proceedings of the International Workshop on Site Response*, Yokosuka, Japan, Vol. **2**, 1996; 185–199.
10. Seed HB, Idriss IM. *Soil moduli and damping factors for dynamic response analyses*. Earthquake Engineering Research Report *EERC 70–10*, University of California, Berkeley, 1970.
11. Bendat JS, Piersol AG. *Engineering Application of Correlation and Spectral Analysis*. Wiley. New York, 1980.
12. Elgamal A-W, Zeghal M, Parra E. Liquefaction of reclaimed land in Kobe, Japan. *Journal of Geotechnical Engineering*, ASCE 1996; **122**(1):39–49.
13. Press WH, Flannery BP, Teukolsky SA, Vettering WT. *Numerical Recipes. The Art of Scientific Computing*. Cambridge Press: New York, 1988.

